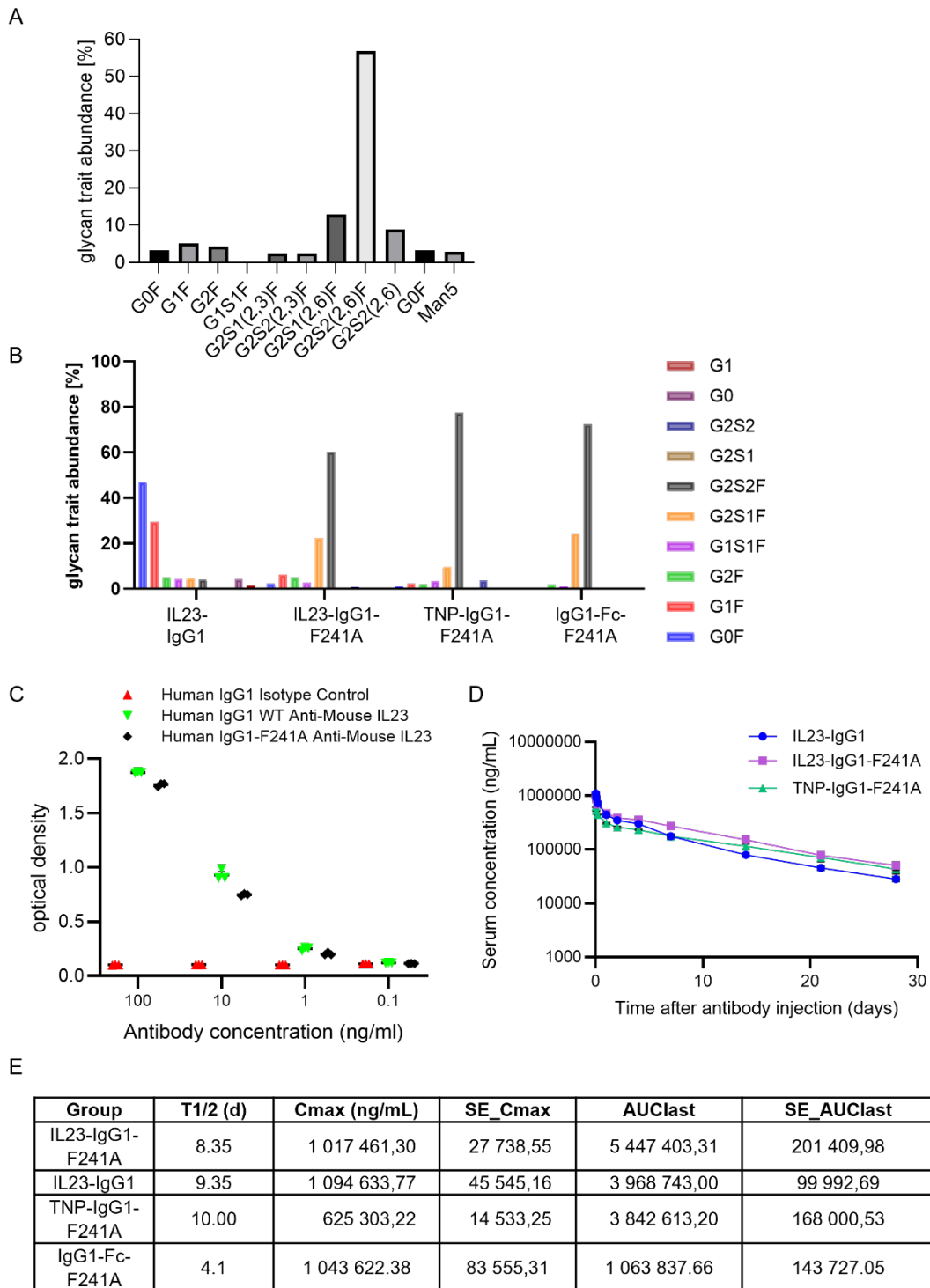


1 Kämpf et al., Supplemental Figures and Methods.



2

3

4 **Figure S1: Characterization of antibody variants used in vivo.**

5 (A) Shown is the relative abundance in percent of the indicated glycan traits in the IL23-

6 IgG1-F241A antibody preparation as determined by hydrophilic interaction liquid

7 chromatography (HILIC) high performance liquid chromatography (HPLC). G: galactose, F:
8 fucose, S: Sialic acid, Man: mannose, 2-3: α 2-3 linked sugar residue, 2-6: α 2-6 linked sugar
9 residue.

10 **(B)** Shown is the relative abundance in percent of the indicated glycan traits in the IL23-IgG1,
11 IL23-IgG1-F241A, TNP-IgG1-F241A, or IgG1-Fc-F241A antibody preparations as determined
12 by nanoLC-ESI-MS analysis. G: galactose, F: fucose, S: sialic acid.

13 **(C)** Shown is the binding (individual data points with mean \pm SEM) of the indicated
14 concentrations (n=3) of IL23-IgG1, IL23-IgG1-F241A, and a TNP-specific isotype control
15 antibody (TNP-IgG1-F241A) to IL23 as determined by ELISA.

16 **(D)** Depicted is the serum concentration (ng/ml) of the indicated antibodies or antibody
17 fragments at different time-points after injection. Shown is the mean \pm SEM of n=6 mice per
18 group.

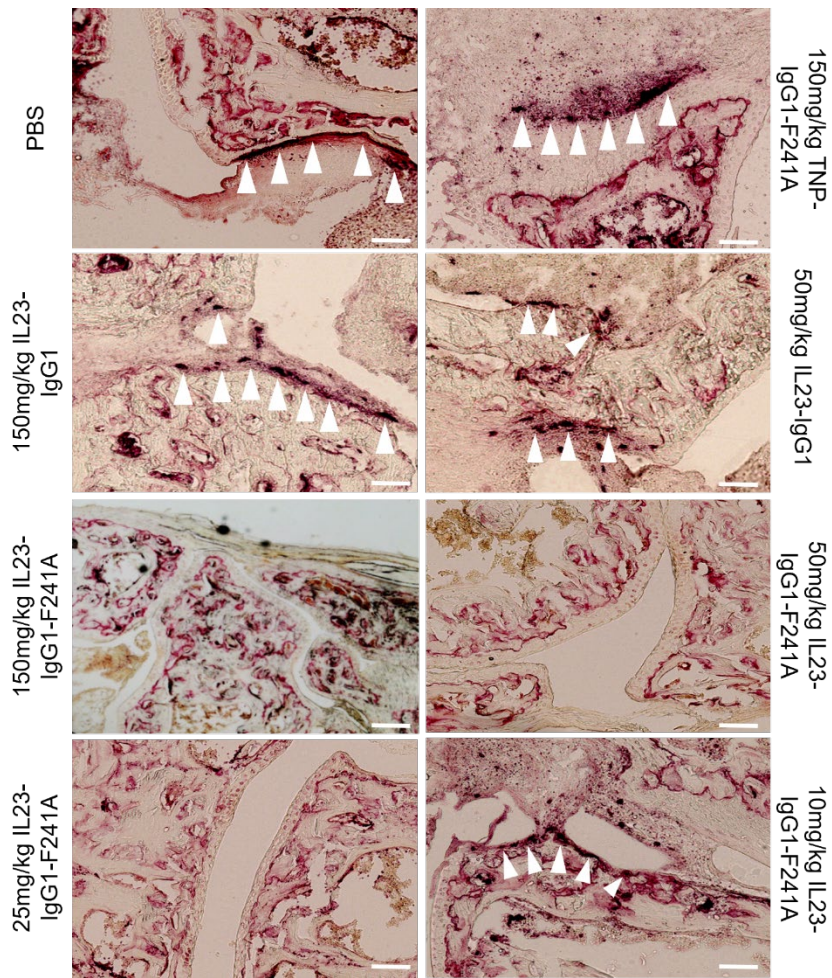
19 **(E)** The table depicts the half-life in days (T_{1/2} (d)), the maximal serum concentration (C_{max}
20 (ng/ml)), the standard error (SE) of C_{max}, the area under the curve of the respective serum
21 concentrations over time (AUC_{last}) and the SE of the AUC_{last} of the indicated human
22 antibodies or Fc-fragments.

23

24

25

26



27

28 **Figure S2: Impact of the IL23-F241A-Fc domain on bone pathology in KBxN mice.**

29 Depicted are representative bone tissue sections of mice treated with PBS or with the
 30 indicated doses of TNP-IgG1-F241A, IL23-IgG1, or IL23-IgG1-F241A antibodies at day 12
 31 after treatment initiation. Sections are stained for tartrate resistant acid phosphatase to
 32 detect osteoclasts. Arrows indicate TRAP+ osteoclasts. Scale bar represents 100µM.

33

34

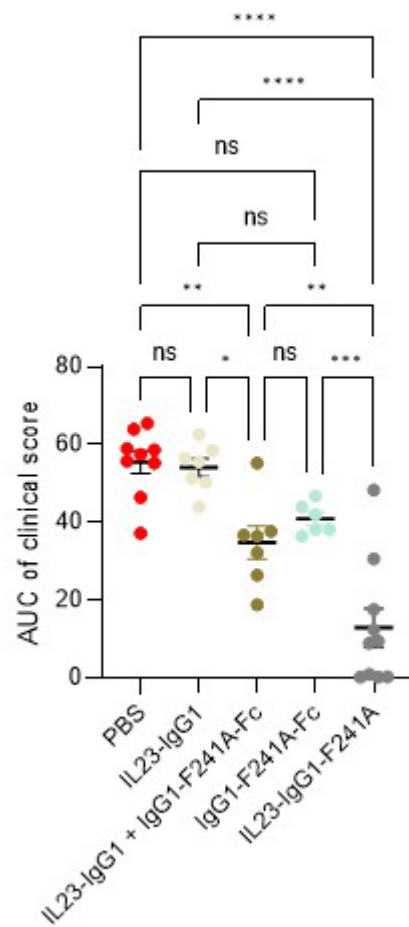
35

36

37

38

39



40

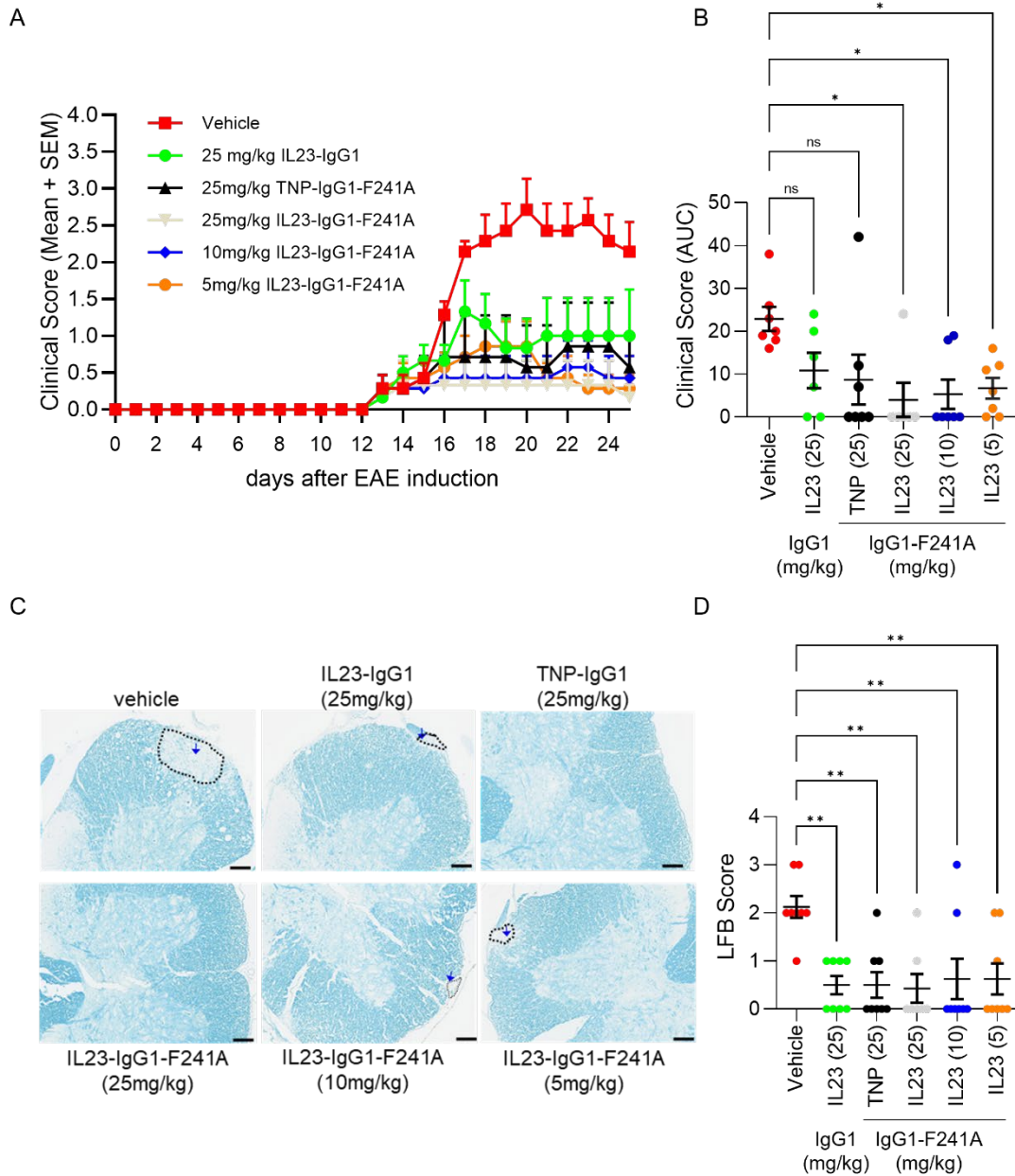
41 **Figure S3: Impact of IL23 antibody intrinsic versus extrinsic F241A Fc-domains on**
 42 **rheumatoid arthritis activity.**

43 Shown is the area under the curve (AUC) of the clinical score of KBxN mice treated with PBS
 44 or 50mg/kg of IL23-IgG1, IL23-IgG1 + IgG1-F241A-Fc, IgG1-F241A-Fc or IL23-IgG1-F241A
 45 (n=5-10 mice per group). Statistically significant differences were identified by using an
 46 ordinary one-way ANOVA and a Tukey's multiple comparison test. *p<0.05, **p<0.01,
 47 ***p<0.001, ****p<0.0001, n.s. not significant.

48

49

50



51 **Figure S4: Immunomodulatory activity of IL23-IgG1 variants in experimental**

52 **autoimmune encephalitis.**

53 **(A)** Shown is the mean clinical score (mean +SEM) of mice (n=6-7) at the indicated time-points
 54 after EAE induction (day 0) followed by treatment with vehicle or the indicated amounts of IL23-
 55 IgG1, IL23-IgG1-F241A, or TNP-IgG1-F241A antibody starting at day 13 after induction of
 56 disease.

57 **(B)** Depicted is the area under the curve (AUC) of the clinical score (mean+SEM) of mice (n=6-
 58 7) treated with the indicated doses of the indicated antibodies or vehicle as a control. Statistical

59 significance was assessed by a mixed-effects analysis with multiple comparisons. * $p < 0.05$, ns:
60 not significant.

61 **(C, D)** Shown are representative LFB stained spinal cord tissue sections **(C)** and the
62 quantification of demyelination (LFB Score, individual data point with median \pm SEM) in the
63 indicated treatment cohorts (n=7-8) **(D)**. Statistical assessment of the data was performed with
64 an ordinary one-way ANOVA with Dunnett's multiple comparison test.** $p < 0.01$. Scale bars in
65 **(C)** represents 100 μ m.

66

67

68 **Supplemental material:**

69

70 **Material and methods:**

71 **Sex as a biological variable**

72 This study focused on female mice as women are more prone to develop severe forms of
73 autoimmune diseases such as multiple sclerosis or rheumatoid arthritis modelled in this study.

74 **Mice**

75 KBxN mice were generated by crossing KRN transgenic mice with NOD-Shild mice as
76 described (1). KBxN mice were bred and maintained at Charles River France. C57BL/6 mice
77 used in the experimental autoimmune encephalomyelitis (EAE) model were provided by
78 Shanghai BK/KY Biotechnology Co., Ltd, Shanghai, China. All mice were maintained
79 according to the rules and regulations of the local animal facilities in France, Germany, and
80 China.

81 **Antibodies**

82 IL23 (p19)-specific human IgG1, human IL23-IgG1-F241A, and human TNP-specific IgG1-
83 F241A antibodies as well as the human IgG1-Fc-F241A antibody fragment (NVG-2089) were
84 produced by ATUM (Newark, California, USA), Just-Evotec Biologics (Seattle Washington,
85 USA), or Evitira (Schlieren, Switzerland). Antibodies or antibody fragments were produced in
86 HD-BIOP3 GS Null Chinese hamster ovary (CHO) K1 cells, stably expressing the respective
87 antibody heavy and light chains. To generate highly sialylated TNP-IgG1-F241A, IgG1-F241A-
88 Fc and IL23-IgG1-F241A antibodies, HD-BIOP3 GS Null Chinese hamster ovary (CHO) K1
89 cells were co-transfected with human ST6GAL1 and human B4GALT1 to add 2,6 linked sialic
90 acid residues (2). ATUM performed cell line construction and single cell cloning. Binding of
91 these antibodies to mouse IL23 p19 was determined by using a sandwich ELISA. In brief, a
92 rabbit anti-mouse p40 antibody (Clone # 2329A, R&D Systems, Minneapolis, MN) was coated
93 to 96 well plates at 1µg/ml overnight at 4°C in 0.2M carbonate/bicarbonate buffer. Wells were

94 then washed and blocked with 5% BSA in PBS-0.05% tween for 1 hour at room temperature,
95 followed by incubation with 0.25µg/ml mouse IL23 (R&D Systems, Minneapolis, MN)
96 suspended in 1% BSA in PBS-0.05% tween for an additional 1 hour at room temperature.
97 Plates were washed and incubated with the human IgG1 anti-mouse IL23 (p19) antibodies
98 (bearing IgG Fc of Fc-F241A) or human IgG1 anti-TNP-F241A antibody at the concentrations
99 indicated on the graph for 1 hour at room temperature. Plates were again washed and
100 antibody binding to mouse IL23 was detected using a 1:100,000 dilution of anti-human IgG-Fc
101 (goat Fab'2) HRP conjugate (Catalogue # 109-036-170, RRID # AB_2783740, Jackson
102 ImmunoResearch Laboratories, West Grove,PA) followed by detection with TMB solution
103 incubated 10 minutes, stopped using H₂SO₄, and read using an optical density of 450nm.

104 **Pharmacokinetic studies of the human antibodies in mice**

105 Female BALB/c mice were dosed intravenously with human IL23-IgG1-F241A, IL23-IgG1,
106 IgG1-F241A-Fc, or TNP-IgG1-F241A antibodies at 50 mg/kg. Blood samples were collected at
107 various time points via retro-orbital bleeding. Serum concentrations of dosed antibodies were
108 measured using an anti-human IgG Fc sandwich ELISA. 96-well plates were coated overnight
109 at 4°C with anti-human IgG, Fc fragment specific capture antibody (Jackson ImmunoResearch
110 Laboratories, West Grove, Pennsylvania) diluted to 1 µg/mL in 0.05 M carbonate/bicarbonate
111 buffer. Plates were washed and blocked with 5% BSA in PBS-0.05% Tween-20 for 2 hours at
112 room temperature. After washing, samples and standards prepared in 1% BSA in PBS-0.05%
113 Tween-20 were incubated with plates for 2 hours at room temperature. Plates were washed
114 and incubated with anti-human IgG Fc-fragment specific HRP conjugated antibody (Jackson
115 ImmunoResearch Laboratories, West Grove, Pennsylvania) prepared at 1:50,000 in 1% BSA
116 in PBS-0.05% Tween-20 for 1 hour at room temperature. Detection was performed using TMB
117 solution incubated for 5 minutes, stopped with H₂SO₄, and optical density was measured at
118 450 nm.

119 **Experimental autoimmune encephalomyelitis (EAE) model system**

120 Weight matched female C57BL/6 mice (6-8 weeks of age) were used in all experiments. To
121 induce EAE, mice were immunized with 200 μ L of MOG peptide (amino acids 35-55) emulsion
122 subcutaneously to induce EAE. In the beginning and 48 hours after immunization, each mouse
123 was administrated intraperitoneally with 250 μ L pertussis toxin (PTX, 1 μ g/mL). Once the first
124 signs of disease became apparent (clinical score below 1), animals were randomly distributed
125 into the following experimental groups and injected every 5th day: vehicle group, IL23-IgG1 (25
126 mg/kg) group, IL23-IgG1-F241A (25 mg/kg), IL23-IgG1-F241A (10 mg/kg), and IL23-IgG1-
127 F241A (5 mg/kg). All antibodies were administered by intravenous injection into the tail vein.
128 During the experiment, the health status of the animals was monitored, the body weight and
129 clinical score were recorded daily by an investigator blinded for the animal groups. The clinical
130 scoring was performed as described. In brief the following symptoms and associated scores
131 were recorded: Score 0: normal mice, no disease characteristics; Score 1: Tail weakness or
132 slight hind limb weakness; Score 2: Tail weakness and hind limb weakness; Score 3: Unilateral
133 hind lib hemiplegia, passive roll over cannot be recovered; Score 4: Complete paralysis of hind
134 limbs, paralysis of forelimbs or weakened muscle strength, accompanied by urinary and fecal
135 incontinence. Score 5: Animals need to be sacrificed due to animal welfare. On day 25 all
136 animals were euthanized with CO₂ and tissue collected for final analysis.

137 **Detection of demyelination in spine tissue of EAE mice.**

138 Demyelination of spine tissue was revealed by luxol fast blue (LFB) staining. In brief, spine
139 tissue was fixed in 10% formalin for 48 hours followed by removal of the backbone. Spinal cord
140 tissue was dehydrated by ascending ethanol solutions and embedded in paraffin. 4 μ m tissue
141 sections were cut with a rotary microtome and dried at 60°C for two hours before staining with
142 0.1% LFB solution overnight at 56°C. Areas with decreased LFB staining were identified as
143 areas with demyelination and assigned scores (Score 0: no demyelination; Score 1: one small
144 area of demyelination; Score 2: 2 or 3 small areas of demyelination; Score 3: 1 or 2 large areas
145 of demyelination; Score 4: extensive demyelination larger than 20% of the white matter area)
146 by an investigator blinded for the samples.

147 **KBxN model system**

148 KBxN mice develop a spontaneous rheumatoid arthritis starting around three weeks of age.
149 All animals with clinical scores below 2 were included in the experiment and randomly assigned
150 to groups. Arthritis was scored by clinical examination as described by an investigator blinded
151 for the experimental groups (2). In brief, the index of all four paws was added: 0 (unaffected),
152 1 (swelling of one joint), 2 (swelling of more than one joint), and 3 (severe swelling of the entire
153 paw), accumulating to a maximum score of 12. Once the first signs of RA became apparent
154 (score below 3), animals were separated into experimental groups and treated with PBS or the
155 respective IL23-specific IgG1 and IgG1-F241A antibodies, the IgG1-F241A Fc, or
156 combinations of antibodies at three day intervals by intraperitoneal injection for twelve days.

157 **Bone histomorphometry**

158 Histological analysis was performed by an investigator blinded for the experimental groups.
159 To quantify bone erosions, osteoclast numbers, and osteoclast size, all tissue was removed
160 from hind legs followed by decalcification for 2 weeks in 14% (wt/vol) EDTA (pH adjusted to
161 7.2 by addition of ammonium hydroxide). 5µm paraffin sections of the tibia and the paw were
162 stained for TRAP and quantification of the different parameters was done by digital image
163 analysis (OsteoMeasure; OsteoMetrics).

164

165 **Analysis of antibody glycosylation**

166 Releasing and labelling N-glycans

167 N-glycan analysis for all proteins was performed by ATUM using standard methodology. N-
168 glycans were released and labeled using the InstantPC kit (Agilent). In brief, 20 mg of intact
169 mAB or fragments and 2ml of Gly-x denaturant was added. The samples were incubated at
170 90°C for 3 minutes, and then the samples were allowed to cool at room temperature for 2
171 minutes. 2ml of N-glycanase was added to each sample, mixed and then incubated at 50°C
172 for 5 minutes. 5ml of InstantPC Dye solution was mixed with the samples and incubated for a

173 further 1 minute at 50°C. To each sample, 150ml of load/wash solution was applied. The
174 samples were transferred to a clean-up plate and vacuum applied. The samples were washed
175 three times with load/wash buffer before the released labeled N-glycans were eluted with
176 100ml of Gly-X Instant PC. The samples were either run immediately on the HPLC-HILIC-FLD
177 or Agilent 6530-QTOF or stored with a foil plate seal at -20°C.

178 HILIC-HPLC Glycan Analysis

179 InstantPC labeled glycans were analyzed by HPLC-FLD on an Agilent 1290 HPLC system with
180 a fluorescence detector (Agilent, USA) using an AdvanceBio Glycan mapping 300A column
181 (1.8mm, 2.1 x 150mm, Agilent) with an increasing ammonium formate linear-gradient (mobile
182 phase A: 100mM ammonium formate pH 4.5 in water; mobile phase B: Acetonitrile) at a flow
183 rate of 0.6mL/min. This column allows detection of 2,3 as well as 2,6 linked sialic acid isoforms.
184 An injection volume of 2ml and a column temperature of 40°C were used. Glycans were
185 detected at a wavelength of 345nm with an excitation wavelength of 285nm. Peaks were
186 integrated using OpenLabs CDS software (Agilent), and the relative glycan compositions were
187 calculated. In conjunction with the samples being run, a dextran ladder (AdvanceBio InstantPC
188 Maltodextrin ladder; Agilent) was run before and after the samples. A ladder was used to
189 calibrate the LC runs and to plot a curve to allocate GU values from retention times. Calculated
190 GU values were compared to a database of reference structures (InstantPC Labeled Glycans,
191 Agilent), allowing N-Glycan to be assigned to each peak. The relative abundance (%Area) of
192 each glycan is expressed as the average of the percentage of the total peak area.

193 Glycan Analysis via Mass Spectroscopy

194 Purified IgG1 N-glycopeptides were analyzed on a Waters nano ACQUITY UPLC system
195 (Waters, Milford, MA, USA) coupled to a Bruker Compact Q-TOF mass spectrometer (Bruker
196 Daltonics, Bremen, Germany) equipped with a Captive Spray ion source. Samples were
197 separated on a C18 nano-LC column (150 mm × 100 µm, 2.7 µm particle size) using a linear
198 gradient of 10–45 % mobile phase B (80 % ACN, 0.1 % TFA) over 7.5 min. Mass spectra were
199 acquired over an m/z range of 600–2000 at a rate of 0.5 Hz. Raw data were processed using

200 Bruker Data Analysis 4.1, and glycopeptide assignments and relative quantification were
201 performed using the semi-automated LacyTools software suite. Manual data curation was then
202 performed to exclude analytes with low mass accuracy, signal-to-noise ratio and isotopic
203 pattern quality from further analysis.

204 **Statistical analysis**

205 Data is shown as Mean \pm SEM and was analyzed by GraphPad Prism with T-Test, One Way
206 ANOVA or Two Way ANOVA (* P<0.05, ** P<0.01, *** P<0.001; ns: not significant).

207 **Study approval**

208 Animal experiments and animal specimen analysis were performed by BioDuro Co., Lt. in
209 Jiangsu, China and at the FAU Erlangen-Nürnberg and were reviewed by institutional review
210 boards in China and Germany (approved under license NIG-FFS-PH-20240809-01 and 55.2.2-
211 2532-2-2170-21).

212 **Data availability**

213 All data and the “Supporting data values” file is available from the corresponding authors upon
214 request.

215 **Acknowledgement**

216 This study was funded by NUVIG therapeutics and grants from the German Research
217 Foundation (DFG-FOR2886-B2, DFG-FOR2953-P3, DFG-TRR369-C01) to FN.

218

219 **Additional references:**

- 220 1. Kouskoff V, Korganow AS, Duchatelle V, Degott C, Benoist C, and Mathis D. Organ-specific
221 disease provoked by systemic autoimmunity. *Cell*. 1996;87(5):811-22.
- 222 2. Ji H, Ohmura K, Mahmood U, Lee DM, Hofhuis FM, Boackle SA, et al. Arthritis critically
223 dependent on innate immune system players. *Immunity*. 2002;16(2):157-68.

224 3. Seeling M, Hillenhoff U, David JP, Schett G, Tuckermann J, Lux A, et al. Inflammatory
225 monocytes and Fcγ receptor IV on osteoclasts are critical for bone destruction during
226 inflammatory arthritis in mice. *Proc Natl Acad Sci U S A*. 2013;110(26):10729-34.

227

228

229